J. Cent. South Univ. (2012) 19: 2926−2932
DOI: 10.1007/s11771-012-1360-3

Springer

Gradient principle of horizontal stress inducing rock burst in coal mine

HE Jiang(何江)[1, 2], DOU Lin-ming(窦林名)[1, 2]

1. State Key Laboratory of Coal Resources and Safe Mining (China University of Mining & Technology), Xuzhou 221116, China;
2. School of Mines, China University of Mining & Technology, Xuzhou 221116, China

Abstract: Based on the stress distribution characteristics of rock burst multiple sites, the criterion of horizontal stress inducing layer dislocation rock burst was established. Accordingly, the influencing factors were analyzed. The analysis results indicate that the stress condition, edge of elastic zone depth, supporting strength, and the friction angle and cohesion among coal stratum, roof and floor are sensitive factors. By introducing double-couple model, the layer dislocation rock burst was explained and the energy radiation characteristics were analyzed. The SOS micro-seismic monitoring system was applied to observe the rock burst hazards about a mining face. The results show that P- and S-wave energy radiations produced by rock burst have directional characteristics. The energy radiation characteristics of the 22 rock bursts occurring on 79Z6 long-wall face are basically the same as theoretical results, that is, the ratio of S-wave energy of sensor 4 to 6 is about 1.5 and that of P-wave is smaller than 0.5. The consistency of the monitored characteristics of the energy radiation theoretically increases with the total energy increasing.

Key words: horizontal stress; rock burst; gradient principle; micro-seismic monitoring; directional characteristic; energy radiation

1 Introduction

Rock burst is one of the main dynamic disasters in deep mining, in recent years, the occurrence frequency and intensity of which increased rapidly and severely restricted mining safety and efficient production.

As the rock burst mechanism determines the formulation and selection of scientific and reasonable control techniques, the research work on it has been continuing without interruption. Initially, the research made a slow progress. In 1965, two representative papers issued by COOK [1−2] made a breakthrough in research and provided the need of experimental base and theoretical analysis of rock burst. His work of using rigid testing machine to study the post-failure behavior of rock set the foundation of the theory of energy release rate (ERR) and the stiffness theory [3]. Afterwards, COOK et al [4] further improved ERR theory in 1966 and PETUKHOV [5] classified rock burst hazards on the base. LINKQV [3] thought the rock burst is a stability problem caused by the softening and rheological behavior. Recently, the mechanics and mathematics greatly promoted the progress of rock burst research [6−11]. The introduction of fractal theory to the study of rock burst by XIE and PARISEAU [12] indicated a new aspect in rock burst research.

Traditionally, the vertical stress was mainly studied in inducing rock burst, while the horizontal stress was ignored. As analyzed, coal normally gets horizontal velocity bursting from coal body in the process of rock burst, so the horizontal stress makes a major role and cannot be neglected.

Since the 1950s, the micro-seismic monitoring method has presented a rapid development. As the early monitoring equipment was regional earthquake network [13], the monitoring accuracy was low. In recent years, many countries developed small-scale seismic monitoring network, which dramatically improved the monitoring accuracy and precipitated a better monitoring result [14−18].

This work concentrated on the role of horizontal stress in inducing rock burst, established the gradient principle of horizontal stress inducing rock burst and applied the micro-seismic monitoring system to observe and analyze the characteristics of energy.

2 Establishment of principle

2.1 Criterion of horizontal stress gradient inducing rock burst

As shown in Fig. 1, the coal body around roadway

Foundation item: Project(2012LWB63) supported by the Fundamental Research Funds for the Central Universities, China; Project(SZBF2011-6-B35) supported by the Priority Acadamic Program Development of Jiangsu Higher Education Institutions (PAPD), China
Received date: 2011−10−10; **Accepted date:** 2012−03−13
Corresponding author: DOU Lin-ming, Professor, PhD; Tel: +86−13952261972; E-mail: lmdou@cumt.edu.cn

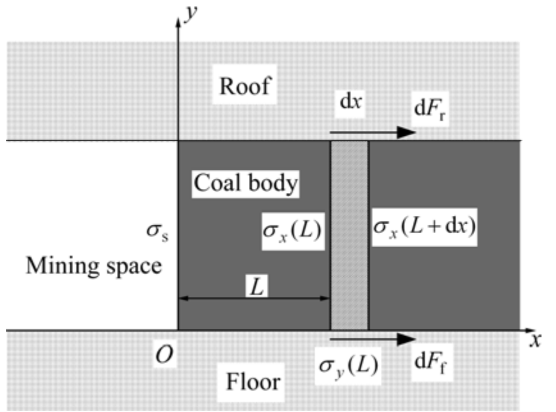

Fig. 1 Stress analysis of coal element

or mining face is under the plane strain stress state. In the direction parallel to the coal wall, a unit length coal mass can be taken for stress analysis. The coal element, that is dx in width, will be analyzed.

If the vertical stress distribution functions of roof and floor are $\sigma_{y,\,\mathrm{r}}(x)$, $\sigma_{y,\,\mathrm{f}}(x)$; the horizontal stress distribution function of coal is $\sigma_x(x, y)$; the coal seam thickness is h; the horizontal sheer stresses between coal and roof and that between the coal and the floor are F_r and F_f, respectively, the density of coal is ρ; and the horizontal displacement of coal is u, the dynamic equilibrium equation can be written as

$$[\bar{\sigma}_x(L)-\bar{\sigma}_x(L+\mathrm{d}x)]h+\mathrm{d}F_\mathrm{r}+\mathrm{d}F_\mathrm{f}=\rho h\frac{\mathrm{d}^2u}{\mathrm{d}t^2}\mathrm{d}x \tag{1}$$

where

$$\bar{\sigma}_x(x)=\frac{\int_0^h\sigma_x(x,y)\mathrm{d}y}{h} \tag{2}$$

Integrally calculating on both ends of Eq. (1) from 0 to L, the following result can be obtained:

$$-h[\bar{\sigma}_x(L)-\sigma_\mathrm{s}]+F_\mathrm{r}+F_\mathrm{f}=\rho hLa \tag{3}$$

where a is the horizontal acceleration of coal element. Suppose the friction angle between the coal and the roof and that between coal and floor are φ_r and φ_f, respectively, and cohesions are C_r and C_f, respectively. If the coal element needs to achieve equilibrium, then F_r and F_f should satisfy the following condition:

$$F_\mathrm{r}\le F_\mathrm{r,max}=\int_0^L[C_\mathrm{r}+\sigma_{y,\,\mathrm{r}}(x)\cdot\tan\varphi_\mathrm{r}]\mathrm{d}x \tag{4}$$

$$F_\mathrm{f}\le F_\mathrm{f,max}=\int_0^L[C_\mathrm{f}+\sigma_{y,\,\mathrm{f}}(x)\cdot\tan\varphi_\mathrm{f}]\mathrm{d}x \tag{5}$$

where

$$\sigma_{y,\,\mathrm{r}}(x)+\rho gh=\sigma_{y,\,\mathrm{f}}(x) \tag{6}$$

Variables F_r and F_f can always automatically adjust their values to maintain the balance of coal body.

In consideration of coal seam's thickness belonging to minimal value relative to mining depth, $\sigma_x(x, y)$ can be considered as symmetric about $y=h/2$. Then, the following result can be deduced as

$$F_\mathrm{r}=F_\mathrm{f}\le\min(F_\mathrm{r,\,max},F_\mathrm{f,\,max}) \tag{7}$$

Supposing that

$$F_\mathrm{C,\,max}=\min(F_\mathrm{r,\,max},F_\mathrm{f,\,max}) \tag{8}$$

Comparing Eqs. (4) and (5), $F_\mathrm{C,\,max}$ can be expressed as

$$F_\mathrm{C,max}=C_\mathrm{C}L+\tan\varphi_\mathrm{C}\int_0^L\sigma_{y,\mathrm{C}}(x)\mathrm{d}x \tag{9}$$

where $F_\mathrm{C,\,max}$ means the critical horizontal stress between the layers of layer dislocation; C_C, φ_C and $\sigma_{y,\mathrm{C}}(x)$ are the cohesion, friction angle and vertical stress distribution function of x, respectively. $F_\mathrm{C,\,max}$ could be judged according to the roof and floor's features and vertical stress distribution. Combining Eq. (3) with Eq. (9), the condition of coal form coal wall to the depth of L occurring layer dislocation can be deduced:

$$[\bar{\sigma}_x(L)-\sigma_\mathrm{s}]h>2C_\mathrm{C}L+2\tan\varphi_\mathrm{C}\int_0^L\sigma_{y,\,\mathrm{C}}(x)\mathrm{d}x \tag{10}$$

where σ_s refers to the support strength on the coal wall surface. Let

$$\bar{\sigma}_{y,\mathrm{C}}(L)=\frac{\int_0^L\sigma_{y,\mathrm{C}}(x)\mathrm{d}x}{L} \tag{11}$$

where $\bar{\sigma}_{y,\,\mathrm{C}}(L)$ is the vertical equivalent uniform stress on coal seam interface of section L. Then, Eq. (10) can be simplified as

$$\frac{\bar{\sigma}_x(L)-\sigma_\mathrm{s}}{L}>\frac{2[C_\mathrm{C}+\bar{\sigma}_{y,\mathrm{C}}(L)\tan\varphi_\mathrm{C}]}{h} \tag{12}$$

The left of Eq. (12) expresses exactly the average gradient of equivalent uniform horizontal stress from coal wall to L, which can be expressed by $\bar{\sigma}_{\mathrm{g},\,x}(L)$, that is

$$\bar{\sigma}_{\mathrm{g},\,x}(L)=\frac{\bar{\sigma}_x(L)-\sigma_\mathrm{s}}{L} \tag{13}$$

Finally, the coal layer dislocation criterion can be expressed as

$$\bar{\sigma}_{\mathrm{g},\,x}(L)>\frac{2[C_C+\bar{\sigma}_{y,\,\mathrm{C}}(L)\tan\varphi_\mathrm{C}]}{h} \tag{14}$$

Equation (14) is also the criterion of horizontal stress gradient inducing rock burst.

2.2 Stress analysis around mining space

As shown in Fig. 2, the coal body around mining space will present as fracture, plastic, elastic and the original stress zones from outside to inside under the

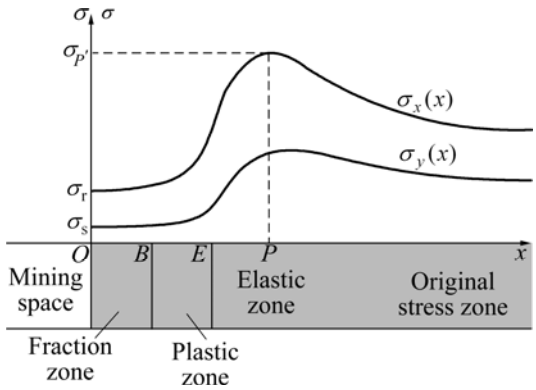

Fig. 2 Stress distribution of coal body

effect of mining concentrated stress. The width and depth of these zones are influenced by the original stress, concentrated stress, strata mechanics, and the interface features between coal and roof and that between coal and floor. So, the accurate values are difficult to be expressed by analysis methods.

The horizontal stress in the elastic zone increases rapidly before the peak stress point. The layer dislocation depth L should be

$$|\overline{OE}| < L < |\overline{OP'}| \tag{15}$$

Research indicates that the peak abutment generally is 2−3.5 times as the mining height [18] apart from coal wall.

2.3 Process and influencing factors

The stress testing and practice indicate that the horizontal stress has no certain relation with the vertical stress. Some mines have a high horizontal stress, while the others have a high vertical one. The following will take hydrostatic stress condition for example to analyze the process and characteristics of horizontal stress gradient inducing rock burst. The relationship between horizontal and vertical stress is [19]

$$\sigma_x = \frac{\mu}{1-\mu}\sigma_y \tag{16}$$

where μ is Poisson ratio of coal. Then,

$$\bar{\sigma}_x(L) = \frac{\mu}{1-\mu}\bar{\sigma}_{y,\mathrm{C}}(L) \tag{17}$$

According to Eqs. (13) and (17), the average stress gradient can be represented as

$$\bar{\sigma}_{\mathrm{g},x}(L) = \frac{\mu}{(1-\mu)L}\bar{\sigma}_{y,\mathrm{C}}(L) - \frac{\sigma_\mathrm{s}}{L} \tag{18}$$

Recording right side of Eq. (14) as $\bar{g}_\mathrm{C}$, then,

$$\bar{g}_\mathrm{C} = \frac{2\tan\varphi_\mathrm{C}}{h}\bar{\sigma}_{y,\mathrm{C}}(L) + \frac{2C_\mathrm{C}}{h} \tag{19}$$

Therefore, regard $\bar{\sigma}_{y,\mathrm{C}}(L)$ as a variable and draw a curve chart on the basis of Eqs. (18) and (19), the intersection point of curves is the critical of layer dislocation rock burst, as shown in Fig. 3.

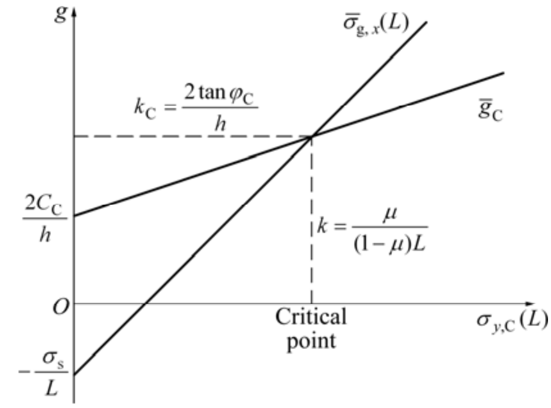

Fig. 3 Critical horizontal stress gradient of rock burst

The occurrence of layer dislocation rock burst depends on the intercept and slope of the two curves. These four parameters are affected by the six physical parameters of μ, L, σ_s, h, φ_C and C_C. The influences were analyzed separately as below.

1) Poisson ratio μ

According to Eq. (18), it is likely to induce layer dislocation rock burst as slope k increases with Poisson ratio increasing. Since Poisson ratio is inherent characteristic of coal, it is only to judge the occurring possibility by μ, but it is difficult to the control rock burst by changing it.

2) Layer dislocation depth L

Its value can only be confirmed after rock burst occurred. But according to Eq. (15), L has a certain value range. L decreases and the occurring possibility of layer dislocation increases with k increasing. If there is no value of L to cause $k>k_\mathrm{C}$, the layer dislocation rock burst would not occur as the vertical stress increases. Noteworthy, as shown in Fig. 4(a) the following situation will cause L to decrease suddenly to induce layer dislocation rock burst:

① Supporting structure losing effectiveness;

② Mining and advancing work;

③ Coal dynamically destroyed and stripping away from coal body;

④ The roadway expansion.

3) Coal wall supporting strength σ_s

It belongs to a minimum value compared with vertical and horizontal stresses. But it can maintain the broken coal to be at home position with stable and make deep coal to be under three-dimensional stress condition, which can maintain the stability of adjacent rock mass. As shown in Fig.4(b), when $k>k_\mathrm{C}$ and k closes to k_C, increasing σ_s can obviously enhance the layer dislocation

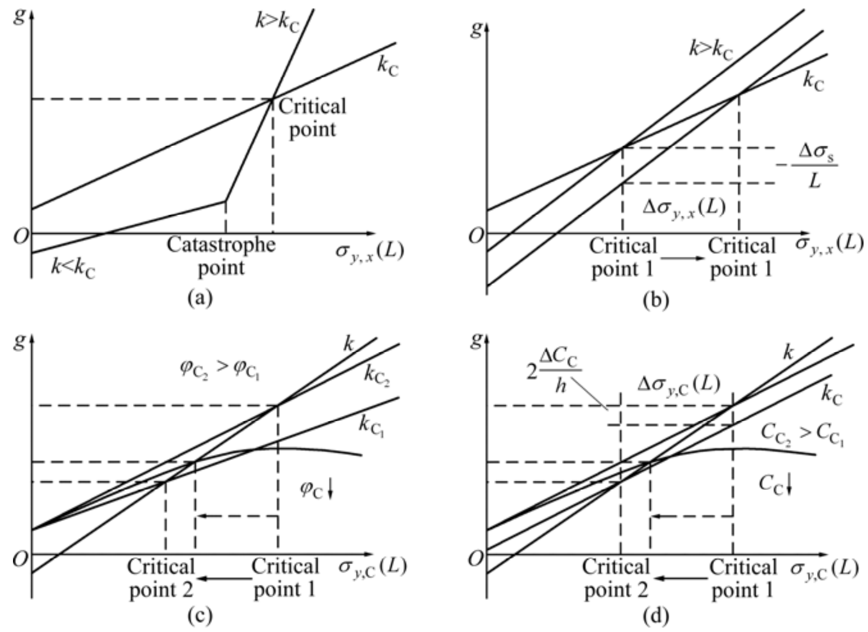

Fig. 4 Analytical process of layer dislocation rock burst: (a) Rock burst induced by L suddenly decreasing; (b) Critical point increasing rapidly with σ_s increasing; (c) Critical point decreasing with φ_C decreasing; (d) Critical point decreasing with C_C decreasing

critical.

4) Coal seam thickness h

It is the inherent attribute of coal seam and cannot be changed. However, according to the layer dislocation criterion, it is possible to determine the dangerous state of rock burst. According to Eq. (14), k_C decreases with h increasing, namely, the possibility of rock burst increases with the thickness of coal seam increasing.

5) Interfacial friction angle φ_C

As shown in Fig. 3, k_C increases with φ_C increasing. As shown in Fig. 4(c), while the stress condition increases to a certain degree, the asperities on the interface between layers will change to yield stage and begin to fracture in the form of shearing, and the interfacial friction angle φ_C will decrease. As shown in Fig. 4(c), the curve of k_C presents the tendency of gradually decreasing, hence the critical point will reduce and the occurrence of layer dislocation rock burst will be easier.

6) Cohesive force C_C

According to Eq. (19), the changing of C_C will directly cause the critical stress gradient curve $\overline{g}_C$ offset. As shown in Fig. 4(d), when C_C increases the curve offsets upper and the critical stress gradient increases. When the stress condition rises to a certain degree, the fracturing of asperities will lead C_C to decrease and cause k_C to descend, as well as the critical stress gradient curve bends downwards. So, the critical stress gradient will decrease to induce the layer dislocation rock burst.

In brief, rock burst has the ingredient of layer dislocation impact more or less. Besides Poisson ratio μ of coal body and coal seam thickness h, the other four parameters are sensitive ones.

3 Micro-seismic in-situ monitoring

3.1 Focal mechanism of layer dislocation rock burst

Layer dislocation rock burst can be explained as the double-couple model [20], the moment tensor of which is symmetrical and can be written as

$$\boldsymbol{M}^{\mathrm{DC}}=\begin{bmatrix}0 & 0 & 1\\ 0 & 0 & 0\\ 1 & 0 & 0\end{bmatrix} \tag{20}$$

The model schematic diagram is shown in Fig. 5.

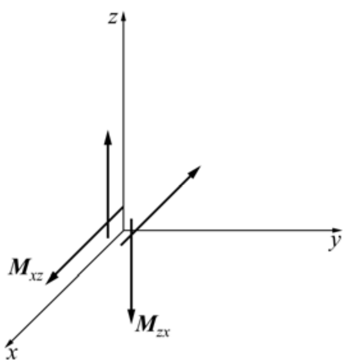

Fig. 5 Double-couple model of layer dislocation rock burst

The far field energy radiation pattern is

$$\begin{cases} R^{\mathrm{P}}=\sin 2\theta\cos\varphi \\ R^{\mathrm{SV}}=\cos 2\theta\cos\varphi \\ R^{\mathrm{SH}}=-\cos\theta\sin\varphi \end{cases} \tag{21}$$

The total amplitude of S-wave is

$$|R^{\mathrm{S}}|=\sqrt{\cos^2 2\theta\cos^2\varphi+\cos^2\theta\sin^2\varphi} \quad (22)$$

where θ is the angle between dislocation plane and radiation aspect projected in the vertical planar layer that is parallel to dislocation aspect. φ is the angle between radiation aspect and the vertical planar layer is parallel to dislocation aspect. P- and S-wave energy radiation patterns are shown in Fig. 6.

As shown in Fig. 6, the energy radiation of layer dislocation rock burst has directionality. θ of the predominant direction of P-wave energy transmitting is ±45°, and the energy decreases with the direction deviating away, while θ of the predominant direction of S-wave is 0° or 90°.

3.2 In-situ monitoring analysis

According to the focal mechanism of layer dislocation rock burst, the theoretical process can be confirmed by the micro-seismic monitoring of the directionalities of P- and S-wave energy transmittings. The applied micro-seismic monitoring system SOS is shown in Fig. 7.

In 79Z6 long-wall face mining process in Taoshan Coal Mine, 23 rock bursts occurred when advancing across the high stress area formed by pillar of upper coal seam, 22 in which occurred on face and one in roadway. As shown in Fig. 8, six sensors of the system have good monitoring condition of 79Z6 face. Sensors 4 and 6 are near to the region of rock bursts concentration, while sensors 8, 11, 14 and 15 are far apart, and separated from the region by F6 fault. In order to avoid the influence of propagation, sensors 4 and 6 are selected for analysis.

Set the seismic source as the origin of coordinate system, the normal unit vector dislocation direction is i, the normal unit vector is parallel to the plane of coal seam pointing to the upper end of mining face is j, and the other one is k, so as to establish the vector space. Supposing the vector pointing to sensor P is $\boldsymbol{p}$, and then the $\boldsymbol{p}$ projection vector on i−k plane can be written as

$$\boldsymbol{p}_{i,k}=(\boldsymbol{P}\cdot i)i+(\boldsymbol{P}\cdot k)k \quad (23)$$

Then,

$$\cos\theta=\frac{\boldsymbol{p}_{i,k}\cdot i}{|p_{ik}|} \quad (24)$$

$$\cos\varphi=\frac{\boldsymbol{p}_{i,k}\cdot\boldsymbol{P}}{|\boldsymbol{p}_{i,k}||\boldsymbol{P}|} \quad (25)$$

As the seismometers of the seismic monitoring system are vertical single component ones, the transferred

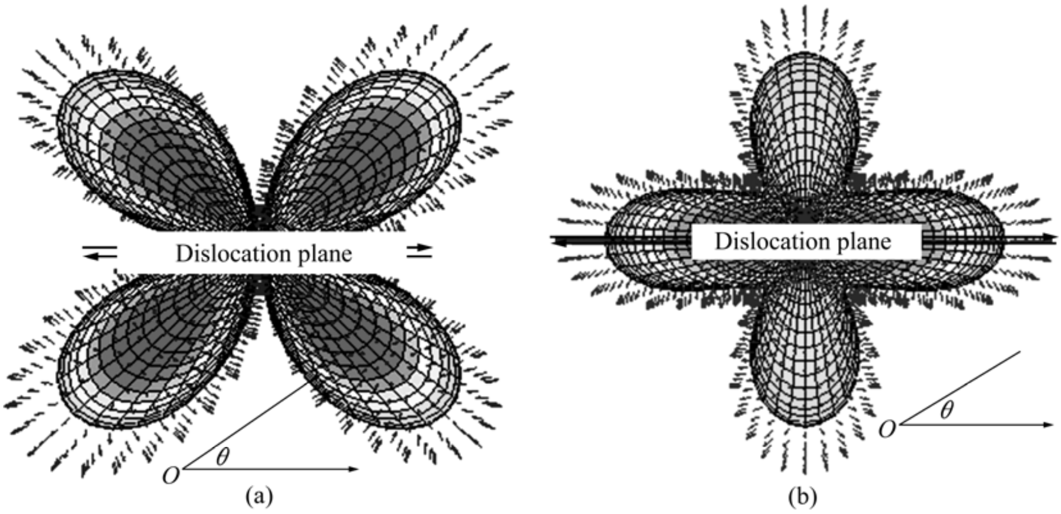

Fig. 6 Energy radiation patterns of layer dislocation rock burst: (a) P-wave energy; (b) S-wave energy

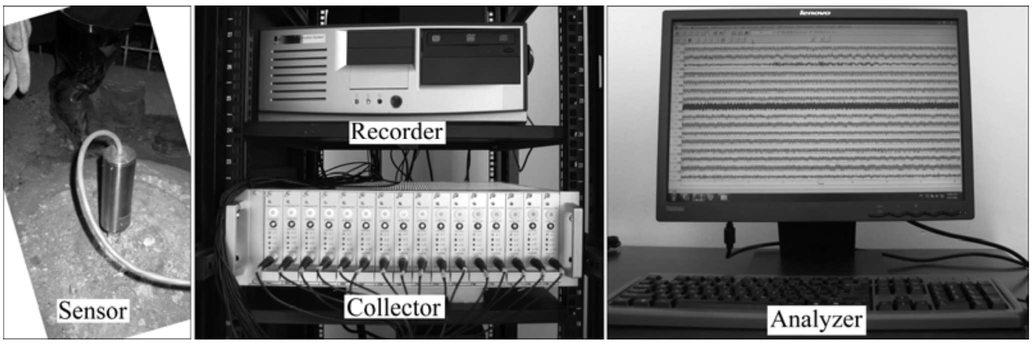

Fig. 7 Photos of SOS micro-seismic monitoring system

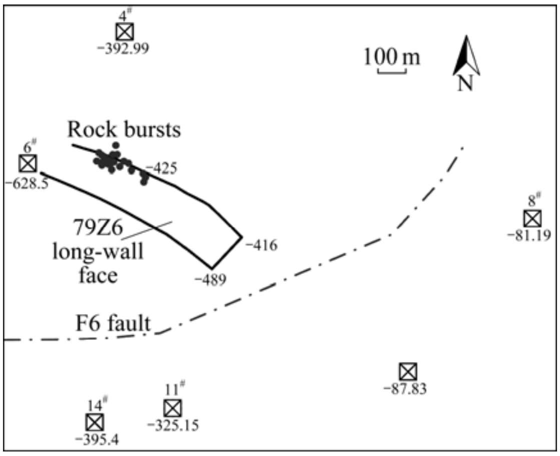

Fig. 8 Distribution of seismic sensors around rock bursts

energy observed by the system on vertical component can be calculated by Eqs. (26) and (27).

$$\begin{cases} R_z^{\mathrm{P}} = [(\boldsymbol{P} \cdot z)/|\boldsymbol{P}|]R^{\mathrm{P}} \\ R_z^{\mathrm{SV}} = (k \cdot \boldsymbol{v}_z)R^{\mathrm{SV}} \\ R_z^{\mathrm{SH}} = (\boldsymbol{l} \cdot \boldsymbol{v}_z)R^{\mathrm{SH}} \end{cases} \tag{26}$$

$$|R_z^{\mathrm{S}}| = \sqrt{(R_z^{\mathrm{SV}})^2 + (R_z^{\mathrm{SH}})^2} \tag{27}$$

where $\boldsymbol{v}_z$ is the vertical unit vector, $\boldsymbol{l}$ is the unit vector that is perpendicular to $\boldsymbol{p}$ and on the i–j plane.

The rock bursts waveforms are similar and one of which is shown in Fig. 9. The maximum P-wave amplitude of sensor 4 is smaller than that of sensor 6, while the maximum S-wave amplitude of sensor 4 is larger than that of sensor 6.

The P-wave arrival time is applied to solve the source location [21], and the waveform integration method is applied to calculate the energy of source by considering the attenuation coefficient. For P- and S-waves separate inconspicuously, the duration time of P- and S-waves was determined approximately as the arrival time deference between P- and S-waves. According to Eqs. (21) to (27), the energy radiation pattern values of sensors 4 and 6 can be obtained.

According to Fig. 10, the conclusion can be drawn:

1) Energy radiation of P- and S-waves has directional characteristic. The S-wave energy radiation recorded by sensor 4 is stronger than that of sensor 6, while the P-wave energy radiation recorded by sensor 6 is stronger than that of sensor 4.

2) The stronger rock burst energy is, the more consistent radiation characteristics with focal mechanism. The process of rock burst is a compound seismic source of coal implosion at the beginning and subsequent layer dislocation. As layer dislocation is the main process of energy release, if the energy released less in dislocation, the rock burst magnitude should be smaller and the energy portion of implosion should be larger. For the implosion energy release is mainly as P-wave, the

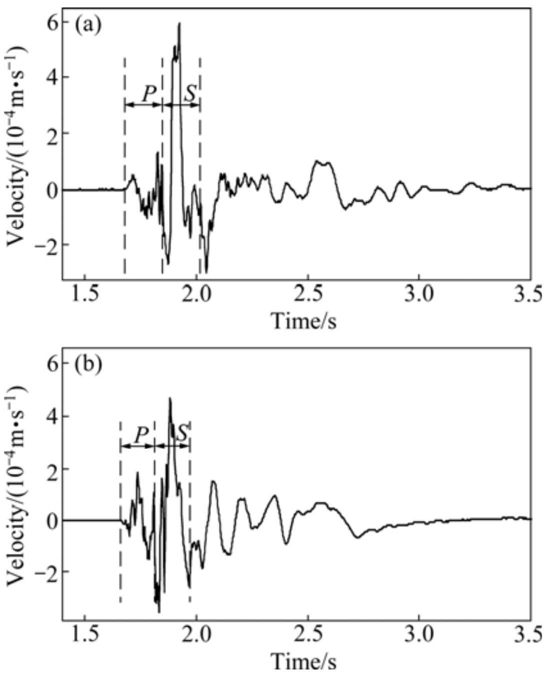

Fig. 9 Typical rock burst waveform: (a) Sensor 4; (b) Sensor 6

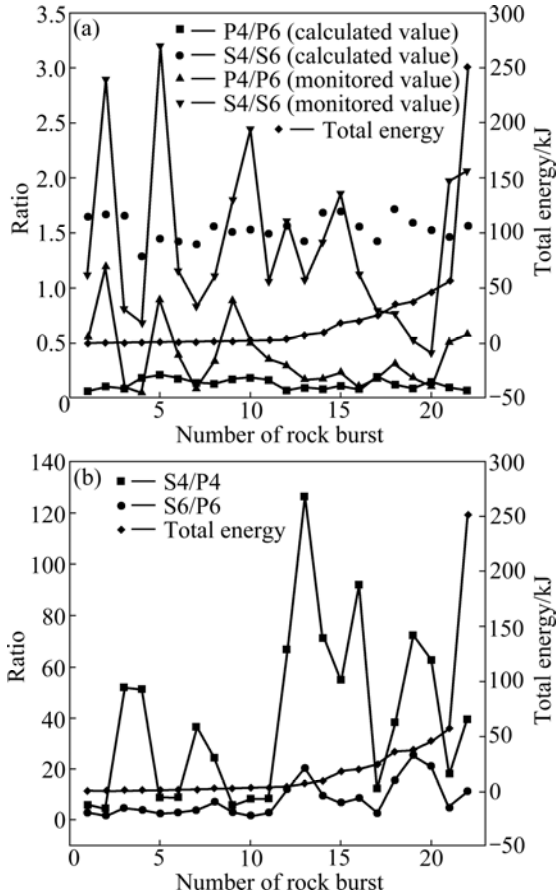

Fig. 10 Comparative analysis of P- and S-wave energies: (a) Comparison of calculated and measured ratios of P- and S-wave energies of sensors 4 to 6; (b) Ratios of P- to S-wave measured energies of sensors 4 and 6

transferred energy is almost the same in every aspect. As shown in Fig. 10(a), when the energy released by the rock burst is small, the ratio of P-wave energy of sensors 4−6 is nearly 1, larger than that of larger energy releasing ones. The ratios of S-wave to P-wave energy of each sensor recorded are shown in Fig. 10(b), which further represents the consistence of rock burst with layer dislocation principle increases with increasing of rock burst energy.

3) The high degree matching of calculated and measured values confirmed the layer dislocation rock burst principle. In considering the case of calculation error, the calculated and monitored results are basically consistent. The conclusion can be drawn that the energy is mainly released in the process of layer dislocation.

4 Conclusions

1) The criterion of horizontal stress gradient inducing layer dislocation rock burst is established, and the influencing factors of which is analyzed. The result indicates that the stress condition, layer dislocation depth L, coal wall supports and protections intensity σ_s, interfacial friction angle φ_C, level cohesive force C_C are the sensitive factors.

2) The layer dislocation rock burst is explained by introducing the double couple model. Accordingly, the energy radiation characteristics of layer dislocation rock burst are deduced. The micro-seismic monitoring results of 22 rock bursts show that the characteristics of rock bursts are consistent with the dislocation rock burst focal mechanism, which indicates that it is the universal of horizontal stress inducing layer dislocation rock burst. The monitoring results also show the consistence of rock burst with layer dislocation principle increases with energy increasing.

References

[1] COOK N G W. The failure of rock [J]. Inr S Rock & Iech Min Sci, 1965, 2(4): 389−403.

[2] COOK N G W. A note on rockbursts considered as a problem of stability [J]. J South Afr Int Min and Metallurgy, 1965, 65(1): 437−446.

[3] LINKQV A M. Rockbursts and the instability of rock masses [J]. Int J Rock Mech Min Sci & Geomech Abstr, 1996, 33(7): 727−732.

[4] COOK N G W, HOEK E, PRETORIUS J P G, ORTLEPP W D, ALAMON M D G. Rock mechanics applied to the study of rockbursts [J]. J South Afr Inst Min and Metallurgy, 1966, 66(1): 435−528.

[5] PETUKHOV I M. Rock bumps in coal mines [M]. Nedra, Moscow, 1972: 1−531. (in Russian)

[6] HU Jian-hua, SU Jia-hong, ZHOU Ke-ping, ZHANG Shi-chao, GU De-sheng. Application and establishment of time-varying mechanical model to induction caving roof [J]. Journal of Central South University: Science and Technlogy, 2007, 38(6): 1212−1218. (in Chinese)

[7] WANG Bin, LI Xi-bing, MA Hai-peng, LI Zhi-guo. Energy source of rock burst based on self-sustaining time-varying structures [J]. Chinese Journal of Geotechnical Engineering, 2010, 32(1): 12−17. (in Chinese)

[8] JIANG Quan, FENG Xia-ting, XIANG Tian-bing, SU Guo-shao. Rockburst characteristics and numerical simulation based on a new energy index: A case study of a tunnel at 2,500 m depth [J]. Earth and Environmental Science, 2010, 69(3): 381−388.

[9] DOU Lin-ming, LU Cai-ping, MU Zong-long, GAO Ming-shi. Prevention and forecasting of rock burst hazards in coal mines [J]. Mining Science and Technology, 2009, 19(5): 585−591.

[10] QI Qing-xin，SHI Yuan-wei，LIU Tian-quan. Mechanism of instability caused by viscous sliding in rock burst [J]. Journal of China Coal Society, 1997, 22(2): 144−148. (in Chinese)

[11] XU Zeng-he, XU Xiao-he, TANG Chun-an. Theoretical analysis of a cusp catastrophe bump of coal pillar under hard rocks [J]. Journal of China Coal Society, 1995, 20(5): 485−491. (in Chinese)

[12] XIE H P, PARISEAU W G. Fractal character and mechanism of rock burst [J]. Int J Rock Mech Min Sci & Geomech Abstr, 1993, 30(4): 343−350.

[13] LI Tie, CAI Mei-feng, CAI M. A review of mining-induced seismicity in China [J]. International Journal of Rock Mechanics and Mining Sciences, 2007, 44(8): 1149−1171.

[14] USZKO M. Monitoring of methane and rockburst hazards as a condition of safe coal exploitation in the mines of Kompania Węglowa SA [J]. Procedia Earth and Planetary Science, 2009, 1(1): 54−59.

[15] TANG L Z, XIA K W. Seismological method for prediction of areal rockbursts in deep mine with seismic source mechanism and unstable failure theory [J]. Journal of Central South University of Technology, 2010, 17(5): 947−953.

[16] HOLUB K, PETRS V. Some parameters of rockbursts derived from underground seismological measurements [J]. Tectonophysics, 2008, 456(1/2): 67−73.

[17] LU Cai-ping, DOU Lin-ming, WU Xing-rong, XIE Yao-she. Case study of blast-induced shock wave propagation in coal and rock [J]. International Journal of Rock Mechanics and Mining Sciences, 2010, 47(6): 1046−1054.

[18] PATYNSKA R, KABIESZ J. Scale of seismic and rock burst hazard in the Silesian companies in Poland [J]. Mining Science and Technology, 2009, 19(5): 604−608.

[19] QIAN Ming-gao, SHI Ping-wu. Mine pressure and ground control [M]. Xuzhou: China University of Mining and Technology Press, 2003: 1−373. (in Chinese)

[20] GIBOWICZ S J, KIJKO A. An introduction to mining seismology [M]. San Diego: Academic Press, Inc., 1994: 95−111.

[21] GONG Si-yuan, DOU Lin-ming, CAO An-ye, HE Hu, DU Tao-tao, JIANG Heng. Study on optimal configuration of seismological observation network for coal mine [J]. Chinese Journal of Geophysics, 2010, 53(2): 457−465. (in Chinese)

(Edited by DENG Lü-xiang)